Chapter 8
Modifications of Photocatalysts by Doping Methods

8.1 Preparation of Visible Light-Responsive TiO_2 Photocatalysts by Chemical Doping Modification Methods

In order to improve the visible light activity of TiO_2, many modification methods have been developed in recent years, like doping impurities, coupling semiconductors, dye sensitization, and so on. After the modification, the visible light-driven TiO_2 can use the solar energy in dealing with the environmental pollution and new energy development. For instance, the dye-sensitized TiO_2 has been widely used in preparing solar cells, owing to its strong visible light absorption ability. In 1991, Michael Grätzel and Brian O'Regan described a photovoltaic cell, created from low- to medium-purity materials through low-cost processes, which exhibited a commercially realistic energy-conversion efficiency [1]. The device is based on a 10-μm-thick, optically transparent film made with TiO_2 particles having a few nanometers in size, coated with a monolayer of dye to sensitize the film for light harvesting. The overall light-to-electric energy conversion is 7.1–7.9% for simulated solar light and 12% for diffuse daylight. The large current densities and high stability of the solar cells based on dye-sensitized colloidal TiO_2 films are making practical applications feasible. Since then, the record of energy conversion for the dye-sensitized TiO_2-based solar cells is constantly improved year by year [2–8]. In 1998, the solar cell based on dye-sensitized mesoporous TiO_2 films converts photons to electric current with a high yield of 33%, which is also achieved by Prof. Michael Grätzel [9]. At present, the photoelectric conversion efficiency of TiO_2-based solar cells has stabilized to be more than 10%, but its cost of manufacturing is still high.

Some other modified visible light-responsible TiO_2 especially the doping-modified TiO_2 also attracted much attention and have been applied to organic pollutant photodegradation and water splitting reaction. Hence, in this section, we would like to introduce the modification methods related to dope trace impurity into TiO_2, including chemical synthesis like high-temperature sintering in an atmosphere,

J. Zhang et al., *Photocatalysis*, Lecture Notes in Chemistry 100,
https://doi.org/10.1007/978-981-13-2113-9_8

wet chemical methods such as sol–gel processes and hydrothermal treatment, spray pyrolysis, and supercritical methods.

These chemical synthesis methods used in doing TiO_2 are summarized in Table 8.1. As can be seen in Table 8.1, all the doped TiO_2 synthesized by different chemical preparation methods have a high photocatalytic activity for the degradation of organic dye pollutants and water splitting. In addition to be divided in different synthesis method, the chemical doping modification on TiO_2 can also be divided into metal doping and nonmetal doping. In metal doping method, a certain amount of metal ions such as Fe^{3+} [10–14], Cr^{3+} [15, 16], Ru^{2+} [17, 18], Ce^{4+} [19, 20], La^{3+} [21–23], V^{5+} [24–26], are introduced into TiO_2 (Table 8.1), as the active "small oxide islands", affecting the lifetime of the photo-formed electrons and holes their-transfer processes, thus affecting the photocatalytic activity of TiO_2. Furthermore, the impurity induced by metal doping into the TiO_2 could efficiently narrow its bandgap and extend the absorption edge into the visible light range. Many studies have demonstrated that metal doping could effectively improve the photocatalytic activity of TiO_2 under the visible light irradiation [27–30]. However, metal doping also showed several drawbacks: thermal instability of doped TiO_2, electron trapping by the metal centers, introduction of the electrons, and hole recombination centers [31]. It is worth mentioning that, in addition to the above traditional impurity metal ion doping, more and more research has focused on the investigation of Ti^{3+} self-doped TiO_2 in recent years [32–36]. Recent research work has found that excessive Ti^{3+} would not easily introduce the electron and hole recombination centers in TiO_2 [33].

On the other hand, nonmetal doping is another technology to modify TiO_2, which could achieve the substitution of lattice oxygen by nonmetal elements [31, 37–39]. Since a work was investigated by Asahi et al. [40] in 2001 in which they reported that nitrogen doping could enhance the photocatalytic activity of TiO_2 for the photodegradation of methylene blue and gaseous acetaldehyde in the visible light irradiation, though the photocatalytic activity in UV light regions decreases. Since then, many researchers have reported about various nonmetal-doped TiO_2, such as N [41, 42], B [43–46], C [21, 47–49], F [50–54], S [55–59], and P [60]. Although nonmetal doping modification could change the band structure of TiO_2 and affect the transfer of electrons and holes, the origin of its visible light photoactivity is still in debate [31], especially the photocatalytic mechanism of nitrogen doping. Recent experimental and theoretical studies suggest that the N doping does not cause the narrowing of the band gap of the TiO_2 but the formation of localized midgap states above the valance band of TiO_2 which is the reason for its enhancing visible light responsiveness and photoactivity [31, 61].

In this section, we mainly introduce and highlight the chemical-synthesized visible light-responsible TiO_2 photocatalysis with doping modification, including metal doping, nonmetal doping, and co-doping modification. The influencing factors on doping modification, the research development of doping and photocatalytic mechanism, and novel investigation of synergistic effect between different elements are also discussed in this section.

Table 8.1 Doping-modified TiO_2 photocatalysts prepared by different chemical methods

Chemical doping method	Doping elements	Precursors	Visible light-driven photocatalysis	Ref.
Sol–gel	N	Ti source: TBOT/TTIP, N source: urea/NH_4Cl/thiourea/ethylmethylamine	Photocatalytic degradation of methylene blue	[62–66]
			Effective agents against both bacteria and stearic acid using a white light source	
	C	Ti source: TTIP/$TiCl_4$	Photodegradation of gaseous toluene or 4-chlorophenol	[67, 68]
		C source: carbon particle ethanol/melamine borate		
	Fe	Ti source: TTIP/TBOT	Photodegradation of active yellow XRG or methyl orange	[10, 29]
		Fe source: $Fe(NO_3)_3 \cdot 9H_2O$		
	B and N	Ti source: TTIP/TBOT	Hydrogen evolution from splitting water	[69–71]
		N source: NH_4OH/urea		
		B source: H_3BO_3		
Hydrothermal	N	Ti source: TiN/$TiCl_4$	Hydrogen evolution from splitting water; photocatalytic degradation of methyl orange	[72, 73]
		N source: TiN/L-lysine		
	Ti^{3+}	Ti source: titanium powder and hydrochloric acid/TBOT and $NaBH_4$	Evolved H_2 under visible light; photodegradation of methyl orange	[33, 74]
	C	Ti source: TBOT/TTIP	Photocatalytic degradation of methyl orange	[75]
		C source: ethanol		
	B and N	Ti source: TTIP/TBOT	Photodegradation for rhodamine B or methyl orange	[76, 77]
		N source: NH_4OH/NH_3/ urea		
		B source: H_3BO_3		
	Ga^{3+}, Y^{3+}, or Nb^{5+}	Ti source: TTIP	Dye-sensitized solar cells (DSSCs).	[78]
		Ga^{3+} source: gallium nitrate		
		Y^{3+} source: yttrium chloride		
		Nb^{5+} source: niobium pentachloride		
	Fe and N	Ti source: TBOT	Photodegradation of rhodamine B	[79]
		N source: NH_4Cl		
		Fe source: $Fe(NO_3)_3$		
	La and C	Ti source: $Ti(SO_4)_2$/TBOT/TTIP	Photodegradation of methyl orange	[21]
		La^{3+} source: lanthanum nitrate		
		C source: glucose		

(continued)

Table 8.1 (continued)

Chemical doping method	Doping elements	Precursors	Visible light-driven photocatalysis	Ref.
Microemulsion	N	Ti source: TBOT, N source: triethylamine, urea, thiourea, and hydrazine hydrate	Photodegradation of rhodamine B and 2,4-dichlorophenol	[41]
	Ag	Ti source: TTIP	Decomposition of phenol	[80]
		Ag source: silver nitrate		
Chemical precipitation	C	Ti source: $TiCl_4$	Photodegradation of 4-chlorophenol	[81]
		C source: tetrabutylammonium hydroxide		
	N	Ti source: TBOT/Ti $(SO_4)_2$	Photodegradation rate of 2,4-DCP or toluene	[42, 64, 82, 83]
		N source: NH_4OH, NH_4NO_3		
	F	Ti source: TTIP	Photocatalytic oxidation of acetone	[84]
		F source: NH_4F		
	Fe	Ti source: K_2TiF_6	Photocatalytic decomposition of bromocresol green	[85]
		Fe source: $FeSO_4{\cdot}7H_2O$		
Chemical deposition	Oxygen vacancies	Ti source: TTIP (CVD method)	Photodegradation of methylene blue	[86]
	Sn^{4+}	Ti source: $TiCl_4$	Photodegradation of phenol	[87]
		Sn^{4+} source: $SnCl_4$		
		Plasma-enhanced chemical vapor deposition (PCVD)		
	Nb, Ta, or F	Ti source: titanium alkoxides/titanium sheets	Photodegradation for methyl orange	[88, 89]
		Nb source: niobium ethoxide		
		Ta source: tantalum ethoxide		
		F source: *t*-butyl fluoride/NH_4F		
		Chemical vapor deposition (PCVD)		
Impregnation	Fe	Ti source: P25/titanate nanotubes	Photodegradation of oxalic acid or photocatalytic oxidation of acetone	[90–92]
		Fe source: $Fe(acac)_3$/$(Fe(NO_3)_3)$/$Fe_2(SO_4)_3$/$FeCl_3$	Photocatalytic degradation of acetophenone	

(continued)

Table 8.1 (continued)

Chemical doping method	Doping elements	Precursors	Visible light-driven photocatalysis	Ref.
	N and Fe	Ti source: $Ti(SO_4)_2$ N source: NH_4OH Fe source: ferric chloride	Photodegradation of methylene blue	[83]
	Co, Cr, Cu, Fe, Mo, V, or W	Ti source: titanium trichloride Co source: Co $(NO_3)_2{\cdot}6H_2O$ Cr source: Cr $(NO_3)_3{\cdot}9H_2O$, Cu source: Cu $(NO_3)_2{\cdot}3H_2O$ Fe source: Fe $(NO_3)_3{\cdot}9H_2O$ Mo source: $(NH_4)_6Mo_7O_{24}{\cdot}4H_2O$ V source: NH_4VO_3 W source: $(NH_4)_6W_{12}O_{39}{\cdot}xH_2O$	Photooxidation of 4-nitrophenol	[93]
High-temperature calcination	H	TTIP/titanium butoxide, H_2 atmosphere at 200/450 °C	Methylene blue decomposition and hydrogen generation	[94–97]
	Ti^{3+}	TTIP, 2-ethylimidazole calcination at 500 °C	High visible light photocatalytic activity for the generation of hydrogen gas from water	[32]
	Ti^{3+} and N	Rutile TiO_2 and NH_4 flow at 500 °C	Extension of the active spectrum and the superior visible light water photooxidation activity	[35]
	C	Ti source: Ti metal sheet C source: CO_2 and steam (H_2O)	Water splitting with a total conversion efficiency of 11% and a maximum photo conversion efficiency of 8.35% when illuminated at 40 milliwatts per square centimeter	[98]
	B	Ti source: $TiCl_4$ B source: BH_3/THF-solution	Photocatalytic decomposition of methyl tertiary butyl ether	[99]
Vacuum activation	Ti^{3+}	TTIP/P25 in vacuum	Photodegradation of methyl orange, phenol, or methylene blue Hydrogen evolution from splitting water	[36, 100]

(continued)

Table 8.1 (continued)

Chemical doping method	Doping elements	Precursors	Visible light-driven photocatalysis	Ref.
	Ti^{3+} and F	Ti source: $Ti(SO_4)_2$ F source: NH_4F	Photodegradation of rhodamine B	[50]
Thermal plasma	H	Ti source: commercial amorphous TiO_2	Photocatalytic methyl orange decomposition and photocatalytic H_2 generation	[101]

8.1.1 Metal Doping Modification

As can be seen from the reaction mechanism of TiO_2 photocatalysis, it can be concluded that an increase in the number of photo-formed electrons and holes participating in the photoredox reaction is the key factor to improve the visible light-responsive TiO_2 photocatalyst's performance. In order to achieve the substantive enhancement of the quantum yield of photocatalytic reaction for TiO_2 in the visible light irradiation, two issues must be overcome. One issue is how to produce much more photo-formed electrons and holes; another issue is how to improve the separation efficiency of electrons and holes. It is well known that appropriate amount of transition metal ions doped into TiO_2 can introduce electron capture centers and change the crystallinity of TiO_2 and then produce some defects, which results in an decrease in photo-formed electron and hole recombination centers [11, 27–30, 33, 34, 102]. Thus, metallic ion doping is recognized as an effective modification method for improving the reactivity of the visible light-responsive TiO_2.

The methods using metallic ions selected for appropriate doping into TiO_2 can be divided into three types. The first type is the transition metal ions. Most early, Choi et al. [103] studied the photoactivity of TiO_2 doped with 21 transition metal ions by using the model reaction of photocatalytic oxidation of chloroform and photocatalytic reduction of carbon tetrachloride. The researchers discovered that the Fe^{3+}, Mo^{5+}, Ru^{3+}, Os^{3+}, Re^{5+}, V^{4+}, and Rn^{3+} ion doping modification is beneficial to the enhancement of photodegradation of chloroform for TiO_2. Recently, Yan et al. [104] synthesized the TiO_2 nanoparticles doped with different content of cerium ion by a sol–gel method. The Ce-doped TiO_2 act as the capture of photo-formed holes and decrease the recombination of photo-generated electrons and holes, leading to better visible light absorption and photocatalytic degradation of methylene blue than pure TiO_2 (Fig. 8.1). Zhang and coworkers have also done many works on the transition of metal-doped TiO_2 and its application to various photocatalytic reactions [14, 15, 19, 20, 24, 29, 105–110]. Iron ion-doped anatase TiO_2 were prepared by hydrothermal hydrolysis and crystallized in octanol–water solution [105]. The results of photodegradation of active yellow XRG dye indicated that the amount of doped iron ion plays a significant role in affecting the photocatalytic activity and iron doped with optimum content enhances the photocatalytic activity, especially under visible light irradiation. When the Fe^{3+}-

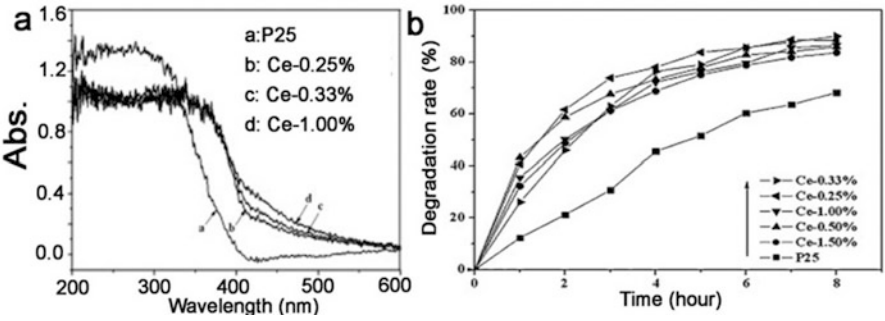

Fig. 8.1 UV–vis absorption spectra of Ce–TiO_2 samples with different Ce ion doping concentrations (**a**). Curves of methylene blue degradation constant by Ce–TiO_2 samples with different Ce ion doping concentrations (**b**) (Reprinted with permission from ref. [104]. Copyright 2015, Elsevier)

doped TiO_2 photocatalysts were prepared by combining sol–gel method with hydrothermal treatment [106], Fe was found to exist in trivalent ionic state and substitute Ti^{4+} in TiO_2, and its concentration was found to decrease from the surface to the deep bulk of TiO_2. As a result, the synthetic method of Fe doping in TiO_2 has a significant influence on the doping structures and concentration. In addition to iron, chromium and vanadium are also widely used as dopant elements into TiO_2. Due to the excitation of 3d electron of Cr^{3+} to the conduction band (CB) of TiO_2, Cr–TiO_2 always shows a good ability for absorbing the visible light to induce the photodegradation of XRG [15]. V^{4+} ions are also successfully incorporated into TiO_2 by flame spray pyrolysis (FSP) technique [24], sol–gel [26, 111], and other chemical methods [25]. V-doping into TiO_2 leads to change the bandgap of TiO_2, leading to an extension of the absorption regions to visible light region, resulting in the improvement of the visible light-driven photocatalytic activity of TiO_2 [26].

The second type is the rare-earth metal doping, and the lanthanide-doped TiO_2 have been accounted for the majority [21, 22, 112–114]. Sun et al. [112] investigated the effects of substitutional La doped on the electronic structures and photocatalytic activity of TiO_2 by the density function theory (DFT) calculation method. Their calculation results indicated that the enhanced absorption in the visible light region for La–TiO_2 was attributed to the adsorptive of La doping rather than the substitutional La. Differently, Anandan et al. [115] believed that the rapid mineralization of monocrotophos over La-doped TiO_2 under the light irradiation could be associated with the suppression of the electrons and holes recombination by La^{3+} doped into TiO_2 and generation of more number of •OH radicals by oxidation of holes. Recently, Zhang and coworkers have studied some other lanthanide metals such as Eu-, Yb-, and Sm-doped TiO_2 and their photocatalytic activities under the visible light irradiation [116–118]. Samarium-doped TiO_2 (Sm–TiO_2) was successfully prepared via a chemical coprecipitation method. The curve in the Sm_{3d} XPS spectrum was found to fit into two peaks [118]. The peak at 1084.3 eV corresponds to the bond of Sm–O. And another peak at 1082.2 eV corresponds to the bond of Sm–O–Ti. Although the ionic radius of Sm^{3+} (1.08 Å) is bigger than the ionic radius

of Ti^{4+} (0.68 Å) and the Sm^{3+} ions cannot enter into the lattice of TiO_2, however, Ti^{4+} ions may enter into the lattice of the Sm_2O_3 leading a change in the electronic field of Sm^{3+} and an increase in the electron density and decrease in the binding energy of Sm^{3+}. Well-ordered mesoporous TiO_2 doped with ytterbium was also successfully synthesized by an evaporation-induced self-assembly process [116]. The Yb dopant was beneficial in stabilizing the mesoporous structure and reduces the recombination of photo-generated electrons and holes, being beneficial to its visible light-driven photoactivity. Europium-doped TiO_2 was synthesized by the precipitation–peptization method and used as the photocatalyst to degrade the salicylic acid [117]. The results showed that the doping of Eu was beneficial to the adsorption of salicylic acid and the separation of photo-formed holes and electrons.

In addition to the transition metal ion doping and rare-earth metal ion doping, the studies on some other metal ion-doped TiO_2 can be seen. Stannum doping TiO_2 and Ti (III) self-doping TiO_2 were also reported. The dopant Sn^{4+} substituted Ti^{4+} in the lattice of TiO_2, which was reflected in the lattice expansion in both *a*- and *c*-direction and change in the binding energy [119]. Different from other metal ion doping, the doping of Sn^{4+} in anatase TiO_2 would result in a blue shift of absorption edge and enhance the amount of surface hydroxyl and oxygen vacancies in the UV light region. On the other hand, Sn doping has also been demonstrated as an effective modification method to enhance the visible light response of TiO_2 [120]. Tin would improve the photocatalytic activity of TiO_2 by enhancing the separation rate of photo-generated electrons and holes on the surface of TiO_2. Due to the Fermi level of SnO_2 lower than that of TiO_2, the photo-generated electrons easily transfer from TiO_2 to SnO_2, resulting in a reduction of the number of photo-generated on the surface of TiO_2. In recent years, Ti^{3+}-doped TiO_2 has attracted much interest, since it has been demonstrated to exhibit visible light absorption [121, 122]. Sasikala et al. [122] have found that the surface Ti^{3+} and oxygen vacancies may be responsible for the enhanced visible light absorption of the TiO_2–SnO_2 composite. However, the surface Ti^{3+} and oxygen defects on the TiO_2 are usually not stable enough in air, since the surface Ti^{3+} is easily oxidized into Ti^{4+} by the dissolved oxygen in water [32, 123]. Most research has focused on Ti^{3+} self-doped TiO_2, which exhibits better chemical stability and is active for photocatalytic activity. Zuo et al. [32] have reported a one-step calcination method to synthesize Ti^{3+} self-doped TiO_2 having high stability and found that it exhibits improved visible light absorption and efficient photocatalytic hydrogen production capacity from water under visible light irradiation (Fig. 8.2, top). It has been also reported a vacuum activation method for modifying P25 to obtain Ti^{3+} self-doped TiO_2 with high stability, visible light absorption, and photocatalytic activity under visible light irradiation (Fig. 8.2, bottom) [36]. In addition to the vacuum activation method, a simple one-step solvothermal method with low-cost $NaBH_4$ added as a reductant was also reported to successfully synthesize a series of TiO_2 catalysts self-doped with Ti^{3+} which also exhibited strong visible light absorption and enhanced photocatalytic activity [33].

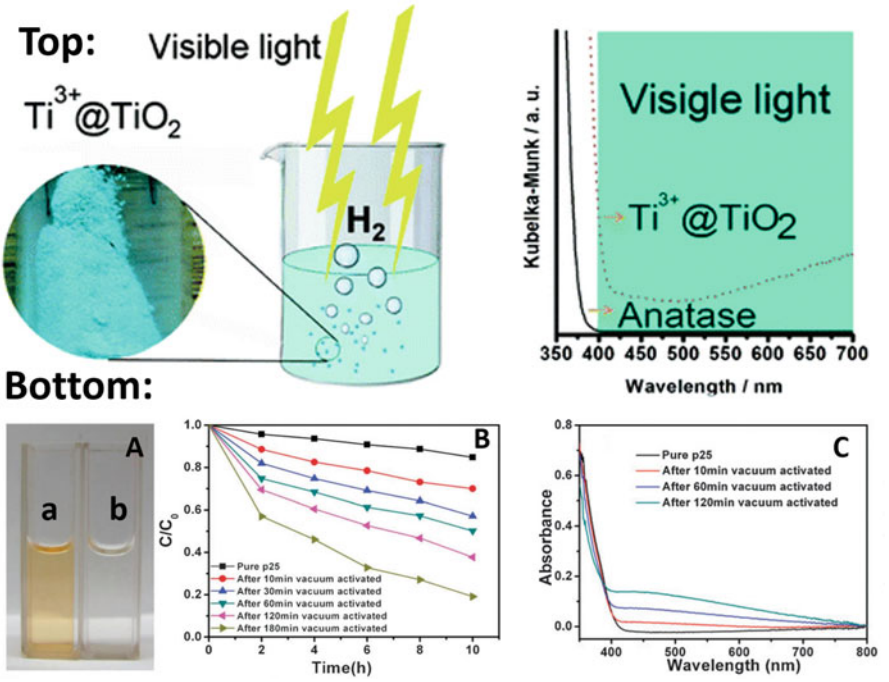

Fig. 8.2 The top figure is the time course of evolved H_2 under visible light (>400 nm) irradiation and the UV−vis diffuse reflectance spectra for commercial anatase TiO_2 (solid line) and Ti^{3+} self-doped TiO_2 (dash line) (the top figures). (Reprinted with permission from ref. [32]. Copyright 2010, American Chemical Society) The bottom figure is (**A**) photooxidation of 5 mg L^{-1} MO before (a) and after (b) visible light (>420 nm) irradiation for 3 h by the sample after vacuum activation for 180 min. (**B**) Photooxidation of 20 mg·L^{-1} phenol under visible light (>420 nm) irradiation for 10 h. (**C**) UV–vis diffuse reflectance spectra for pure P25 and the vacuum-activated samples (Reprinted with permission from ref. [36]. Copyright 2011, Royal Society of Chemistry)

8.1.2 Nonmetal Doping Modification

Although the metal doping modification could promote the absorption of TiO_2 for the visible light, the metallic ions also would induce the poor thermostability of TiO_2 and introduce some recombination centers with an excess doping concentration. Since in 2001 Asahi et al. [50] found that the nitrogen-doped TiO_2 exhibited the visible light absorption and photocatalytic activity, the study on nonmetal doping modification in TiO_2 has been a research hotspot.

Taking into consideration of the poor thermostability caused by the metal doping and the high cost in modification, the increasing number of nonmetal elements is used as the dopant to modify the bandgap of TiO_2 in recent years. Nonmetal doping mainly consists of the N, C, F, B, and other elements having the similar atomic radius with O atom. Among them, nitrogen has attracted much attention and been

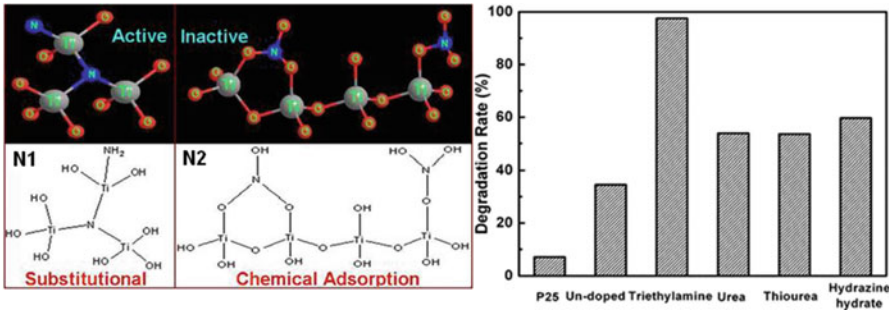

Fig. 8.3 The left figure is the nitrogen forms doped in TiO_2 (Reprinted with permission from ref. [42]. Copyright 2009, Elsevier); the right figure is the photocatalytic activities of TiO_2 prepared from different nitrogen sources with the optimal doping value (Reprinted with permission from ref. [41]. Copyright 2007, American Chemical Society)

widely studied. In some of recent work [51, 52], a new approach to synthesize the N-doped TiO_2 nanocrystals was developed, and the relationship of doped nitrogen species to visible light photoactivity was investigated. It was found that the nitrogen introduced into TiO_2 is beneficial to the visible light photodegradation of 2,4-dichlorophen and the nitrogen species chemically adsorbed on catalyst surface are harmful to the photoactivity, as shown in Fig. 8.3 [42]. Moreover, the nitrogen source also plays an important role in the N doping effect. Urea, triethylamine, thiourea, and hydrazine hydrate all could be used as the nitrogen source to prepare the nitrogen-doped TiO_2 by a microemulsion–hydrothermal method [41]. Among the above nitrogen sources, triethylamine was a more effective nitrogen source, which was used to synthesize the N-doped TiO_2 with the highest visible light photocatalytic degradation of rhodamine B (Fig. 8.3). Yates et al. [124] used NH_3 gas as the nitrogen source to prepare the N-doped TiO_2 with enhanced visible light photoactivity by a calcination method. However, the TiO_2 treated by the N_2 had decreased photoactivity due to the broadening of the bandgap of TiO_2.

In addition to nitrogen, carbon is also demonstrated to be an effective doping element to modify the visible light absorption and photoactivity of TiO_2. Nagaveni et al. [125] successfully prepared the C-doped TiO_2 by using a sol–gel method, which exhibited a high photodegradation of methylene blue under the visible and UV light irradiation. Kamisaka et al. [126] investigated the affection of C doping on the structure and optical property of TiO_2 by the density functional theory (DFT) calculation method. They assumed the carbon atom could substitute four sites of titanium and oxygen to obtain four corresponding C-doping structures. The DFT calculation results indicated that the substitution of C for Ti could not cause the visible light response of TiO_2 because of the formation of titanate anion. On the contrary, the substitution of C for O was beneficial to the visible light absorption of TiO_2 and did not change its crystal structure. Recently, Bai et al. [127] prepared monodisperse, carbon-doped rutile TiO_2 single crystal with exposed (110) facets, which possessed hierarchical structure and highly efficient H_2 generation activity. Yu et al. [128] also fabricated novel carbon self-doped TiO_2 sheets with exposed

(001) facets by a hydrothermal treatment. The C-doped TiO_2 sheets had enhanced absorption in the whole visible light region and a significant redshift at the absorption edges. It was also showing a high photocatalytic degradation of methylene blue under the visible light irradiation. Lin et al. [129] prepared a visible light-driven C-doped mesoporous TiO_2 films by a sol–gel method combined with a hydrothermal treatment. The C-doped TiO_2 film had high surface area and excellent photodegradation of dye reactive brilliant Red X-3B in the UV and visible light irradiation.

Fluorine-doped TiO_2 as one of the widespread modified methods has attracted much more attention in recent years, but conventional F-doped TiO_2 is hard to effectively achieve the enhanced UV and visible light photoactivity, and its photocatalytic mechanism still remains controversial [130–132]. In previous work, NH_4F was used as a hydrophobic modifier, and isopropanol was used as the solvent to prepare super-hydrophobic mesoporous MCF loaded with fluorinated TiO_2 nanoparticles [50], through a simple one-step solvothermal method (Fig. 8.4, top). The prepared catalyst exhibited permanent and excellent super-hydrophobic property, high adsorption capacity, and photocatalytic activity for rhodamine B degradation (Fig. 8.4, bottom). However, through the solvothermal method, the F ion could only adsorb on the surface of the catalyst but not be introduced into TiO_2 lattice. Many researchers also have reported the F-doped TiO_2 having high photocatalytic activity [50, 132]. And the standard substitutional of TiO_2 with F is similar to F-doped SnO_2, with generation of impurity levels close to the conduction band [133–135]. However, its electronic structures and photocatalytic mechanism are still unclear. It has been demonstrated that F substitution for lattice O could not introduce impurity level inside TiO_2 band gap, as well as shift its absorption edge into visible region by the first-principles calculation [136]. That is because of the absence consideration of F substitution for oxygen vacancy during the calculation process. Some studies have reported that F substitution for oxygen vacancy could introduce acceptor impurity level inside ZnO or SnO_2 bandgap [137, 138]. Hence, it was concluded that the achievement of abundant fluorine substitution for lattice oxygen vacancy played a very important role in the diminishing of vacancy-induced recombination sites and the introduction of impurity level inside the TiO_2 bandgap [53].

Compared with the abovementioned nonmetal elements, the study on boron doping in TiO_2 is relatively rare in recent years. In some studies, it was suggested that the boron doping in TiO_2 could lead to a redshift of the absorption band of TiO_2 to the visible light region, because of the overlapping of the impurity levels caused by boron with the 2p electronic states of oxygen [139, 140]. By contrast, some other studies reported that the boron incorporation into TiO_2 lattice could induce a blue shift rather than redshift due to the decrease of the crystal size [141, 142]. The quantization effect of the crystal size would result into a blue shift of absorption band to the UV light region. Even so, the boron has still been used as an important co-dopant together with other nonmetals for modification of TiO_2. Hence, more and more researchers began to study the co-doping modification of boron with other elements in TiO_2 [70, 77, 143, 144].

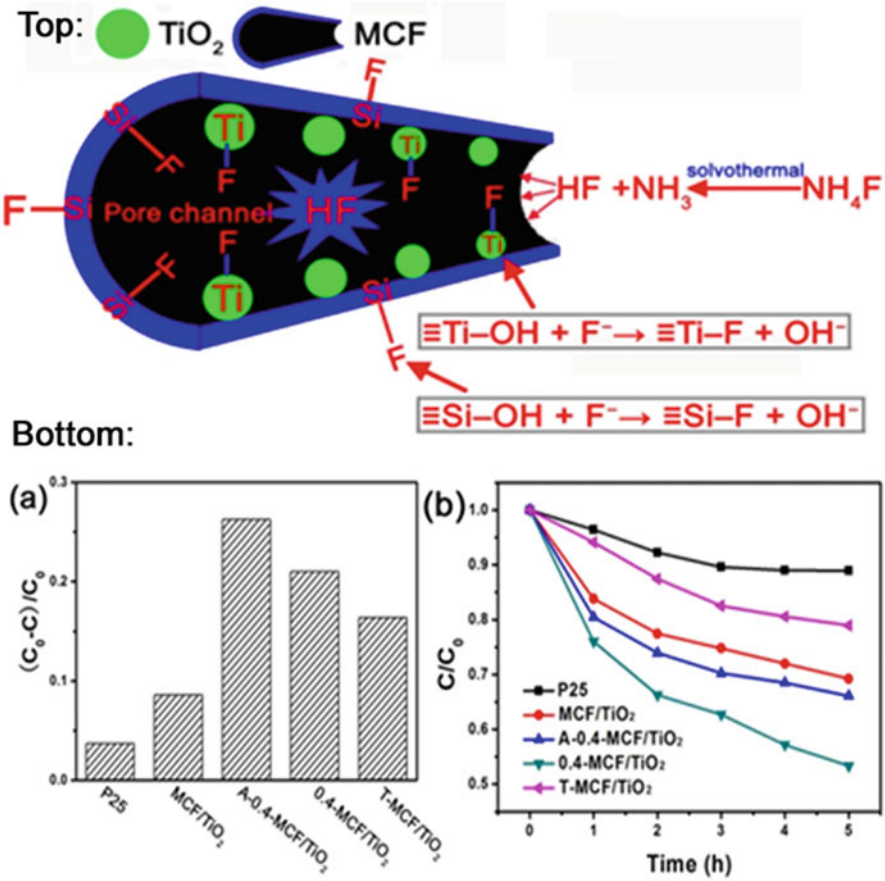

Fig. 8.4 The top figure is the schematic diagram of the fluorination reaction that occurred in the pore channels of MCF; the bottom figure is adsorption capacities of RhB (20 mg/L, catalyst concentration: 0.25 g/L) on different samples (**a**); visible light photocatalytic activities of different samples (**b**) (Reprinted with permission from ref. [50]. Copyright 2012, Elsevier)

8.1.3 Co-doping Modification

In order to further improve the photocatalytic activity of TiO_2 and make effective use of sunlight in visible light region, multicomponent modified TiO_2 such as co-doped with different elements has attracted much more attention in the photocatalysis fields. Some studies found that co-doped TiO_2 with appropriate elements could exhibit a much higher photocatalytic activity than single-doped catalyst, because of the existence of synergistic effect of doped elements which could promote the visible light absorption and facilitate the separation efficiency of photo-formed electrons and holes [11, 25, 35, 76, 77, 112, 116, 145, 146]. Herein, we will focus on summary of the research status of the co-doping modification on TiO_2

photocatalyst in recent years, the modification mechanism of co-doping, and the synergistic effect existing in the co-doped TiO_2.

According to the band theory of semiconductors, the conduction band of TiO_2 semiconductors is mainly determined by the Ti3d orbital energy level, and the valence band mainly depends on the energy level of O2p orbital. Compared with the O2p orbital, nonmetal elements such as N, C, S, and P have the 2p orbital with relatively high energy levels; hence, it is possible to enhance the visible light photocatalytic activity of TiO_2 by the doping N, C, S, P, and other nonmetal elements, due to the increase of electric potential of valence band by the partial substitution of impurity dopants for lattice oxygen.

Compared with other nonmetallic element co-doping modification, nitrogen co-doped with other nonmetal modification is very important, owing to the significant synergistic effect for visible light response. Cong et al. [147] proposed that the energy level of N doping could connect with the states of C doping and facilitate the overlap of C1s and N1s with the VB states of TiO_2, as shown in Fig. 8.5. The co-doping of N and C further narrowed the band gap of TiO_2 and improved the visible light photocatalytic activity of TiO_2 [147]. Meanwhile, boron has also been used as an important co-dopant together with nitrogen for co-doping modification of TiO_2 [69, 76, 77, 99, 143]. In et al. [99] and Liu et al. [76] proposed that B and N co-doped TiO_2 show a high UV and visible light photocatalytic activity, probably due to the existence of a synergistic effect between boron and nitrogen by the formation of Ti–B–N structure at the catalyst surface. However, there is still no detailed illustration of the B–N synergistic effect and its effect on the photocatalytic activity of TiO_2. Xing et al. [77] have illustrated the exact role of synergistic effect in optical absorbance and photocatalytic activity of B and N co-doped TiO_2. Various co-doped TiO_2 was systematically prepared by using the double hydrothermal

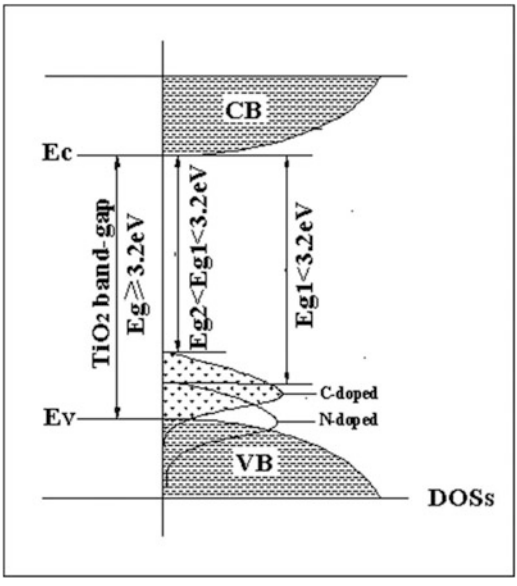

Fig. 8.5 Mechanism for photocatalytic degradation of organic pollutants over C–N–TiO_2 photocatalyst under visible light irradiation (Reprinted with permission from ref. [31]. Copyright 2010, Royal Society of Chemistry; and reprinted with permission from ref. [147]. Copyright 2006, Chemical Society of Japan)

method. Different new bonds were determined to form on the surface of TiO_2 when the order of boron and nitrogen addition was changed, and they could significantly affect the photoactivities of the materials. The abovementioned experimental results are further illustrated by the DFT calculation. Gombac et al. [148] found that the surface N doping did not appreciably modify the TiO_2 structures and texture, and boron incorporation in TiO_2 indeed inhibited the TiO_2 crystallite growth and increased the surface area of TiO_2. Only when B was present in excess with respect to N, a remarkable photoactivity improvement could be obtained. DFT calculation method was used to interpret the observed behavior. And the B in molar excess with respect to N led to the generation of Ti^{3+} sites, which might further induce the generation of reactive superoxide species. Different from the surface bond structures and the reactive Ti^{3+} sites induced by B and N co-doping, Czoska et al. [70] considered that the lattice center (labeled $[NOB]^{\cdot}$) based on the presence of interstitial N and B atoms both bound to the same lattice oxygen ion could introduce an energy level near the edge of VB of TiO_2. $[NOB]^{\cdot}$ can easily trap one electron to produce a diamagnetic center at about 0.4 eV above the top of the VB (Fig. 8.6), which can contribute to the visible light photoactivity.

Recently, nitrogen and sulfur co-doped TiO_2 was successfully immobilized on the surface of nitride Ti substrate, which exhibited high photodegradation of methylene blue in the visible light irradiation [149]. It was estimated that N and S co-doping in the anodic TiO_2 narrowed the band gap of TiO_2 and enhanced its visible light absorption and photocatalytic activity. In order to eliminate the recombination centers induced by the nonmetal doping in TiO_2 nanoparticles, Yang et al. [150] synthesized the fluorine and sulfur co-doped mesoporous TiO_2. The ability to control the morphology and chemical composition of the mesoporous TiO_2 could be beneficial to improve the light-harvesting capacity and decrease the recombination centers. The F and S co-doping in TiO_2 can redshift the threshold of the TiO_2 absorption into the visible light region and improve the photocatalytic efficiency for the degradation of organic pollutants. As well as our previous work, some nonmetal co-doped TiO_2 are successfully synthesized for the photodegradation of organic dyes under the visible light irradiation. N- and F co-doped TiO_2 microspheres were prepared by ethanol solvothermal method [151]. It was found that the co-doped catalyst with mesoporous structure exhibited a significant synergistic

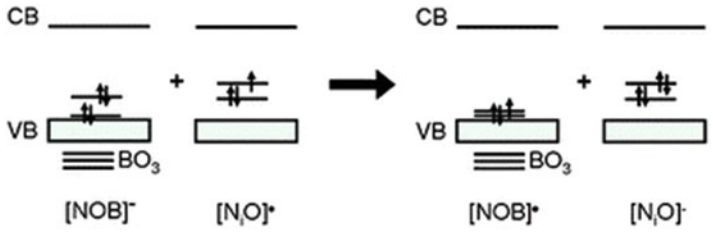

Fig. 8.6 Schematic representation of interplay between the $[NOB]^{\cdot}$ and $[NiO]^{\cdot}$ centers in N–B co-doped TiO_2 (Reprinted with permission from ref. [70]. Copyright 2011, Royal Society of Chemistry)

effect of N and F doping, which led to the high photocatalytic activity of the degradation of AO7 in the visible light irradiation. Moreover, carbon and boron co-doped TiO_2 were also synthesized firstly by the gel–hydrothermal method [144], that is, prepared through sol–gel process followed by hydrothermal in the glucose solution. The experimental results indicated that the coke carbon generated on the co-doped catalyst surface acted as a photosensitizer and had a photosensitization effect under the visible light. And the boron doping could effectively narrow the band gap of TiO_2, which induced the easier transition of photo-formed electrons from the boron dopant level to the Ti^{3+} level. The synergistic effect of B and C is responsible for its excellent visible light photocatalytic activity.

Either metal doping or nonmetal doping, they both will change the electric structure of TiO_2 and create a new doping level inside the band gap of TiO_2. Because of the different position of doping level in TiO_2, it is generally considered that the doping level induced by the substitution of metallic ions for Ti^{4+} is close to the CB of TiO_2. And the impurity level caused by the doping of nonmetallic ions into the oxygen vacancy sites is nearby the VB of TiO_2. These doping levels are located inside the band gap of TiO_2, which can accept the photo-formed electrons from the VB or absorb the photos with longer wavelength and extend the range of absorption spectrum of TiO_2. The synergistic effect between the metal and nonmetal could promote the separation of electrons and holes, resulting into the improvement of the visible light photocatalytic activity of TiO_2.

Generally speaking, the synergistic effect between metal and nonmetal is mainly shown as follows: the nonmetallic ion doping can enhance the absorption of TiO_2 in the visible light region, and the metallic ion doping can introduce traps for electrons and decrease the recombination of electrons and holes. Vanadium and nitrogen co-doped TiO_2 was synthesized by the sol–gel method, and the catalyst showed a high visible light photocatalytic activity for the degradation of RhB [111]. The visible light absorption efficiency of V–N co-doped TiO_2 was better than the V or N single-doped TiO_2, because of the effective narrowing of the band gap induced by the simultaneous incorporation of V and N in TiO_2 lattice, as shown in Fig. 8.7. The energy levels inside the TiO_2 band gap can act as traps for photo-formed holes and electrons thus decrease the recombination between photo-formed charges. The narrowed band gap and enhanced charge separation exhibit synergistic effect to improve the visible light photoactivity of the co-doped TiO_2. Wei et al. [152] considered that the synergistic effect between nitrogen and lanthanum in La and N co-doped TiO_2 was responsible for the high photocatalytic activity. The N doping decreased the band gap of TiO_2 and increased the absorption intensity of TiO_2 in visible light region. And the La^{3+} doping could not only increase the surface area of TiO_2 but also restrain the recombination of electrons and holes, due to the electron capturing capacity of La^{3+}. In order to minimize the role of metallic ions as recombination centers, Kim and coworkers synthesized boron and iron co-doped TiO_2 using a modified sol–gel method, and the presence of boron and iron caused a redshift in the absorption band of TiO_2 [153]. Cong et al. [79] also have successfully prepared the nanosized TiO_2 catalyst co-doped with nitrogen and iron, which exhibited a higher photocatalytic activity than the single doping catalyst under the

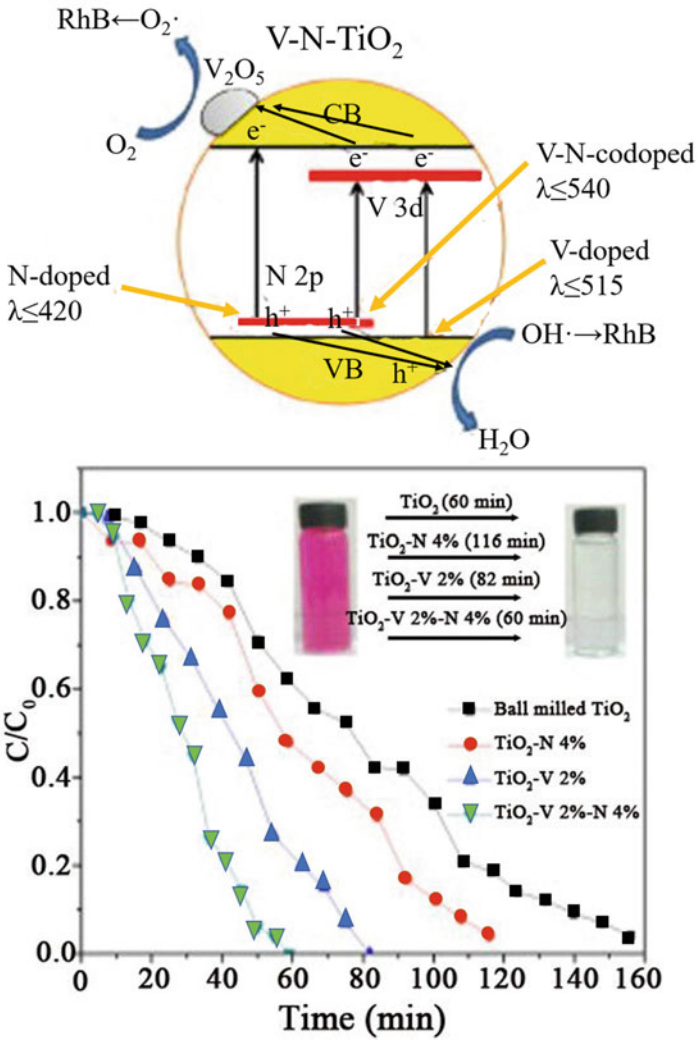

Fig. 8.7 Schematic diagram for photocatalytic degradation of RhB dye over V2–N4-co-doped TiO_2 photocatalyst under light irradiation. And the comparison of photocatalytic degradation of RhB under visible light source in the presence of undoped, V2-doped, N4-doped, and V2–N4-co-doped TiO_2 powders (Reprinted with permission from ref. [111]. Copyright 2012, Elsevier)

visible light irradiation. Xing et al. [21] prepared the highly dispersed carbon and lanthanum co-doped TiO_2 crystals with exposed (001) facets by using glucose as the carbon-doping source and (001)-facet-controlling agent through a simple one-step hydrothermal method. The C doping was responsible for the strong absorption in the visible light region, and the La doping acted as the electron capture center. The

synergistic effect of C and La is the reason for the high visible light photocatalytic activity of the co-doped TiO_2.

However, in addition to the abovementioned synergistic effect, there are also some other forms of synergistic effects between metal and nonmetal, such as the increase of the surface active species including the hydroxyl groups and hydrogen peroxide in TiO_2. The role of surface hydroxyl groups and hydrogen peroxide is mainly including two aspects: one is involving in the reaction with the photo-formed holes to generate the hydroxyl radicals; another function is changing the adsorption forms of reactant and acting as the active center to influence the photocatalytic reaction of the reactant molecules. Wei and coworkers found that the content of hydroxyl groups on the surface of sulfur and iron co-doped TiO_2 was increasing, as can be seen in the XPS characterization [154], which is beneficial to its visible light photocatalytic activity. The difference of surface –OH between pure TiO_2 and single-doped TiO_2 is very small, while the amount of surface –OH on Fe and S co-doped TiO_2 is much higher than single-doped catalyst, resulting from the synergistic effect between Fe and S. The increase of surface –OH is in favor of the enhancing of the photoactivity. Gomathi Devi et al. [155] prepared the Ag and nitrogen co-doped TiO_2 by grinding sol–gel titania with urea followed by a photoreduction process. The as-prepared Ag–$TiO_{2-x}N_x$ exhibited much higher visible light photocatalytic activity than the single nitrogen doped TiO_2, which can be accounted to the synergistic effect of Ag loading with N doping. Strongly interacting electron accepting species of hydrogen peroxide at the catalyst surface are acting as the surface states enabling inelastic transfer of electrons from the CB to the oxidizing species. Additionally, the synergistic effect also can be shown as the electrons transfer between the co-dopant states. Hoang et al. [35] reported a synergistic effect involving Ti^{3+} and nitrogen in TiO_2 nanowire arrays, which exhibited an enhanced water photooxidation performance in the visible light irradiation. The authors proposed a reversible electron transfer between the paramagnetic bulk species of N (N_b) and Ti^{3+} centers forming the diamagnetic bulk species of N_b^- and Ti^{4+}. That means the existence of interaction between Ti^{3+} and N in TiO_2 (Fig. 8.8). The lower oxidation states of the substitutional N in the co-doped TiO_2 might be resulted from the electron transfer form Ti^{3+}. Because of the Columbic repulsion, the lower oxidation states of N in co-doped TiO_2 have higher energy than that of the N single-doped TiO_2, thus enabling excitation with photons of longer wavelengths.

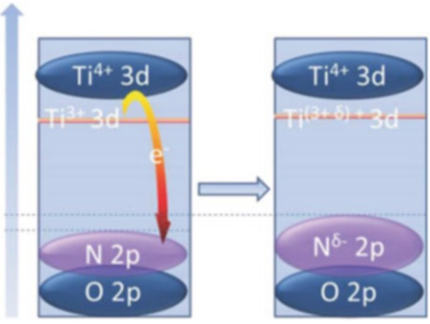

Fig. 8.8 Proposed mechanism for the interaction between Ti^{3+} and substitutional N (Reprinted with permission from ref. [35]. Copyright 2012, American Chemical Society)

References

1. O'Regan B, Gratzel M (1991) A low-cost high-efficiency solar cell based on dye-sensitized colloidal TiO_2 films. Nature 353:737–740
2. Ito S, Chen P, Comte P et al (2007) Fabrication of screen-printing pastes from TiO_2 powders for dye-sensitised solar cells. Prog Photovolt Res Appl 15(7):603–612
3. Ito S, Zakeeruddin SM, Humphry-Baker R et al (2006) High-efficiency organic-dye-sensitized solar cells controlled by Nanocrystalline-TiO_2 electrode thickness. Adv Mater 18 (9):1202–1205
4. Kuang D, Brillet J, Chen P et al (2008) Application of highly ordered TiO_2 nanotube arrays in flexible dye-sensitized solar cells. ACS Nano 2(6):1113–1116
5. Nazeeruddin MK, Humphry-Baker R, Liska P et al (2003) Investigation of sensitizer adsorption and the influence of protons on current and voltage of a dye-sensitized nanocrystalline TiO_2 solar cell. J Phys Chem B 107(34):8981–8987
6. Nazeeruddin MK, Pechy P, Renouard T et al (2001) Engineering of efficient panchromatic sensitizers for nanocrystalline TiO_2-based solar cells. J Am Chem Soc 123(8):1613–1624
7. Wang P, Zakeeruddin SM, Comte P et al (2003) Enhance the performance of dye-sensitized solar cells by co-grafting amphiphilic sensitizer and hexadecylmalonic acid on TiO_2 nanocrystals. J Phys Chem B 107(51):4336–14341
8. Zukalova M, Zukal A, Kavan L et al (2005) Organized mesoporous TiO_2 films exhibiting greatly enhanced performance in dye-sensitized solar cells. Nano Lett 5(9):1789–1792
9. Bach U, Lupo D, Comte P et al (1998) Solid-state dye-sensitized mesoporous TiO_2 solar cells with high photon-to-electron conversion efficiencies. Nature 395(6702):583–585
10. Zhu JF, Chen F, Zhang J et al (2006) Fe^{3+}-TiO_2 photocatalysts prepared by combining sol-gel method with hydrothermal treatment and their characterization. J Photochem Photobiol A Chem 180(1):196–204
11. Yang Y, Tian CX (2012) Effects of calcining temperature on photocatalytic activity of Fe-doped sulfated Titania. Photochem Photobiol 88(4):816–823
12. Shi JW, Zheng JT, Hu Y et al (2007) Influence of Fe^{3+} and Ho^{3+} co-doping on the photocatalytic activity of TiO_2. Meter Chem Phys 106(2):247–249
13. Zhu J, Zheng W, He B et al (2004) Characterization of Fe-TiO_2 photocatalysts synthesized by hydrothermal method and their photocatalytic reactivity for photodegradation of XRG dye diluted in water. J Mol Catal A Chem 216(1):35–43
14. Tong T, Zhang J, Tian B et al (2008) Preparation of Fe3+-doped TiO_2 catalysts by controlled hydrolysis of titanium alkoxide and study on their photocatalytic activity for methyl orange degradation. J Hazard Mater 155(3):572–579
15. Zhu JF, Deng ZG, Chen F et al (2006) Hydrothermal doping method for preparation of Cr^{3+}-TiO_2 photocatalysts with concentration gradient distribution of Cr3+. Appl Catal B Environ 62 (3):329–335
16. Anpo M, Takeuchi MJ (2003) The design and development of highly reactive titanium oxide photocatalysts operating under visible light irradiation. J Catal 216(1):505–516
17. Hamzah N, Nordin NM, Nadzri AHA et al (2012) Enhanced activity of Ru/TiO_2 catalyst using bisupport bentonite-TiO_2 for hydrogenolysis of glycerol in aqueous media. Appl Catal A: General 419:133–141
18. Panagiotopoulou P, Kondarides DI, Verykios XEJ (2010) Mechanistic study of the selective methanation of CO OVER ru/TiO_2 catalyst: identification of active surface species and reaction pathways. J Phys Chem C 115(4):1220–1230
19. Yuan S, Chen Y, Shi LY et al (2007) Synthesis and characterization of Ce-doped mesoporous anatase with long-range ordered mesostructure. Mater Lett 61(21):4283–4286
20. Tong TZ, Zhang JL, Tian BZ et al (2007) Preparation of Ce-TiO_2 catalysts by controlled hydrolysis of titanium alkoxide based on esterification reaction and study on its photocatalytic activity. J Colloid Interface Sci 315:382–388

21. Xing MY, Qi DY, Zhang JL et al (2011) One-step hydrothermal method to prepare carbon and lanthanum co-doped TiO_2 nanocrystals with exposed {001} facets and their high UV and visible-light photocatalytic activity. Chem Eur J 17(41):11432–11436
22. Yuan S, Sheng QR, Zhang JL et al (2005) Synthesis of La^{3+} doped mesoporous titania with highly crystallized walls. Microporous Mesoporous Mater 79(1):93–99
23. Gao HT, Liu WC, Lu B et al (2012) Photocatalytic activity of La, Y co-doped TiO_2 nanoparticles synthesized by ultrasonic assisted sol–gel method. J Nanosci Nanotechnol 12 (5):3959–3965
24. Tian B, Li C, Gu F et al (2009) Flame sprayed V-doped TiO_2 nanoparticles with enhanced photocatalytic activity under visible light irradiation. Chem Eng J 151(1):220–227
25. Liu H, Wu Y, Zhang J (2011) A new approach toward carbon-modified vanadium-doped titanium dioxide photocatalysts. ACS Appl Mater Interfaces 3(5):1757–1764
26. Lin WC, Lin YJ (2012) Effect of vanadium (IV)-doping on the visible light-induced catalytic activity of titanium dioxide catalysts for methylene blue degradation. Environ Eng Sci 29 (6):447–452
27. Sajjad S, Leghari SAK, Chen F et al (2010) Bismuth-doped ordered mesoporous TiO_2: visible-light catalyst for simultaneous degradation of phenol and chromium. Chem Eur J 16:13795–13804
28. Wang WJ, Zhang JL, Chen F et al (2010) Catalysis of redox reactions by Ag@ TiO_2 and Fe^{3+}-doped Ag@ TiO_2 core–shell type nanoparticles. Res Chem Intermed 36(2):163–172
29. Yuan XL, Zhang JL, Anpo M et al (2010) Synthesis of Fe3+- doped ordered mesoporous TiO_2 with enhanced visible light photocatalytic activity and highly crystallized anatase wall. Res Chem Intermed 36(1):83–93
30. Cong Y, Tian BZ, Zhang JL (2011) Improving the thermal stability and photocatalytic activity of nanosized titanium dioxide via La^{3+} and N co-doping. Appl Catal B Environ 101 (3):376–381
31. Zhang J, Wu Y, Xing M et al (2010) Development of modified N doped TiO_2 photocatalyst with metals, nonmetals and metal oxides. Energy Environ Sci 3(6):715–726
32. Zuo F, Wang L, Wu T et al (2010) Self-doped Ti^{3+} enhanced photocatalyst for hydrogen production under visible light. J Am Chem Soc 132(34):11856–11857
33. Xing M, Fang W, Nasir M et al (2013) Self-doped Ti3+-enhanced TiO_2 nanoparticles with a high-performance photocatalysis. J Catal 297:236–243
34. Zheng Z, Huang B, Meng X et al (2013) Metallic zinc-assisted synthesis of Ti^{3+} self-doped TiO_2 with tunable phase composition and visible-light photocatalytic activity. Chem Commun 49(9):868–870
35. Hoang S, Berglund SP, Hahn NT et al (2012) Enhancing visible light photo-oxidation of water with TiO_2 nanowire arrays via cotreatment with H_2 and NH_3: synergistic effects between Ti^{3+} and N. J Am Chem Soc 134(8):3659–3662
36. Xing M, Zhang J, Chen F et al (2011) An economic method to prepare vacuum activated photocatalysts with high photo-activities and photosensitivities. Chem Commun 47 (17):4947–4949
37. Liu GL, Han C, Pelaez M, Zhu DW, Liao SJ, Likodimos V, Ioannidis N, Kontos AG, Falaras P, Dunlop PSM, Byrne JA, Dionysiou DD (2012) Synthesis, characterization and photocatalytic evaluation of visible light activated C-doped TiO_2 nanoparticles. Nanotechnology 23(29):294003
38. Selvam K, Swaminathan M (2012) Nano N-TiO_2 mediated selective photocatalytic synthesis of quinaldines from nitrobenzenes. RSC Adv 2(7):2848–2855
39. Zhang W, Yang B, Chen J (2012) Effects of calcination temperature on preparation of boron-doped TiO_2 by sol-gel method. Int J Photoenergy 2012:1
40. Asahi R, Morikawa T, Ohwaki T et al (2001) Visible-light photocatalysis in nitrogen-doped titanium oxides. Science 293(5528):269–271
41. Cong Y, Zhang JL, Chen F et al (2007) Synthesis and characterization of nitrogen-doped TiO_2 nanophotocatalyst with high visible light activity. J Phys Chem C 111(19):6976–6982

42. Xing M, Zhang J, Chen F et al (2009) New approaches to prepare nitrogen-doped TiO_2 photocatalysts and study on their photocatalytic activities in visible light. Appl Catal B Environ 89(3):563–569
43. Lu XN, Tian BZ, Chen F et al (2010) Preparation of boron-doped TiO_2 films by autoclaved-sol method at low temperature and study on their photocatalytic activity. Thin Solid Films 519 (1):111–116
44. Wu YM, Xing MY, Zhang JL et al (2010) Effective visible light-active boron and carbon modified TiO_2 photocatalyst for degradation of organic pollutant. Appl Catal B Environ 97 (1):182–189
45. Tang YB, Yin LC, Yang Y et al (2012) Tunable band gaps and p-type transport properties of boron-doped graphenes by controllable ion doping using reactive microwave plasma. ACS Nano 6(3):1970–1978
46. Wang XD, Blackford M, Prince K et al (2012) Preparation of boron-doped porous titania networks containing gold nanoparticles with enhanced visible-light photocatalytic activity. ACS Appl Mater Interfaces 4(1):476–482
47. Wu YM, Zhang JL, Xiao L et al (2010) Properties of carbon and iron modified TiO_2 photocatalyst synthesized at low temperature and photodegradation of acid orange 7 under visible light. Appl Surf Sci 256(13):4260–4268
48. Parayil SK, Kibombo HS, Wu CM et al (2012) Enhanced photocatalytic water splitting activity of carbon-modified TiO_2 composite materials synthesized by a green synthetic approach. Int J Hydrog Energy 37(10):8257–8267
49. Zhong J, Chen F, Zhang JL (2009) Carbon-deposited TiO2: synthesis, characterization, and visible photocatalytic performance. J Phys Chem C 114(2):933–939
50. Xing MY, Qi DY, Zhang JL et al (2012) Super-hydrophobic fluorination mesoporous MCF/TiO_2 composite as a high-performance photocatalyst. J Catal 294:37–46
51. Tosoni S, Fernandez Hevia D, González Díaz Ó et al (2012) Origin of optical excitations in fluorine-doped titania from response function theory: relevance to photocatalysis. J Phys Chem Lett 3(16):2269–2274
52. Liu SW, Yu JG, Cheng B et al (2012) Fluorinated semiconductor photocatalysts: tunable synthesis and unique properties. Adv Colloid Interf Sci 173:35–53
53. Seo H, Baker LR, Hervier A et al (2010) Generation of highly n-type titanium oxide using plasma fluorine insertion. Nano Lett 11(2):751–756
54. Kuwahara Y, Maki K, Matsumura Y et al (2009) Hydrophobic modification of a mesoporous silica surface using a fluorine-containing silylation agent and its application as an advantageous host material for the TiO_2 photocatalyst. J Phys Chem C 113(4):1552–1559
55. Xu P, Xu T, Lu J et al (2010) Visible-light-driven photocatalytic S-and C-codoped meso/nanoporous TiO_2. Energy Environ Sci 3(8):1128–1134
56. Niu Y, Xing M, Tian B et al (2012) Improving the visible light photocatalytic activity of nanosized titanium dioxide via the synergistic effects between sulfur doping and sulfation. Appl Catal B Environ 115–116:253–260
57. Bidaye P, Khushalani D, Fernandes JB (2010) A simple method for synthesis of S-doped TiO_2 of high photocatalytic activity. Catal Lett 134(1–2):169–174
58. Dozzi MV, Livraghi S, Giamello E et al (2011) Photocatalytic activity of S-and F-doped TiO_2 in formic acid mineralization. Photochem Photobiol Sci 10(3):343–349
59. He HY (2010) Solvothermal synthesis and photocatalytic activity of S-doped TiO_2 and TiS_2 powders. Res Chem Intermed 36(2):155–161
60. Yang K, Dai Y, Huang BJ (2007) Understanding photocatalytic activity of S-and P-doped TiO_2 under visible light from first-principles. J Phys Chem C 111(51):18985–18994
61. Di Valentin C, Pacchioni G, Selloni A et al (2005) Characterization of paramagnetic species in N-doped TiO_2 powders by EPR spectroscopy and DFT calculations. J Phys Chem B 109 (23):11414–11419
62. Livraghi S, Paganini MC, Giamello E et al (2006) Origin of photoactivity of nitrogen-doped titanium dioxide under visible light. J Am Chem Soc 128(49):15666–15671

63. Caratto V, Setti L, Campodonico S et al (2012) Synthesis and characterization of nitrogen-doped TiO_2 nanoparticles prepared by sol–gel method. J Sol-Gel Sci Technol 63(1):16–22
64. Dong F, Zhao W, Wu Z et al (2009) Band structure and visible light photocatalytic activity of multi-type nitrogen doped TiO_2 nanoparticles prepared by thermal decomposition. J Hazard Mater 162(2):763–770
65. Hao H, Zhang J (2009) The study of iron (III) and nitrogen co-doped mesoporous TiO_2 photocatalysts: synthesis, characterization and activity. Microporous Mesoporous Mater 121 (1):52–57
66. Jagadale TC, Takale SP, Sonawane RS et al (2008) N-doped TiO_2 nanoparticle based visible light photocatalyst by modified peroxide sol−gel method. J Phys Chem C 112 (37):14595–14602
67. Kim MS, Liu G, Nam WK et al (2011) Preparation of porous carbon-doped TiO_2 film by sol–gel method and its application for the removal of gaseous toluene in the optical fiber reactor. J Ind Eng Chem 17(2):223–228
68. Neville EM, Mattle MJ, Loughrey D et al (2012) Carbon-doped TiO_2 and carbon, tungsten-codoped TiO_2 through sol–gel processes in the presence of melamine borate: reflections through photocatalysis. J Phys Chem C 116(31):16511–16521
69. Gopal NO, Lo HH, Ke SC (2008) Chemical state and environment of boron dopant in B, N-codoped anatase TiO_2 nanoparticles: an avenue for probing diamagnetic dopants in TiO_2 by electron paramagnetic resonance spectroscopy. J Am Chem Soc 130(9):2760–2761
70. Czoska AM, Livraghi S, Paganini MC et al (2011) The nitrogen–boron paramagnetic center in visible light sensitized N–B co-doped TiO_2. Experimental and theoretical characterization. Phys Chem Chem Phys 13(1):136–143
71. Li Y, Ma G, Peng S et al (2008) Boron and nitrogen co-doped titania with enhanced visible-light photocatalytic activity for hydrogen evolution. Appl Surf Sci 254(21):6831–6836
72. Liu G, Yang HG, Wang X et al (2009) Visible light responsive nitrogen doped anatase TiO_2sheets with dominant {001} facets derived from TiN. J Am Chem Soc 131 (36):12868–12869
73. Wang DH, Jia L, Wu XL et al (2012) One-step hydrothermal synthesis of N-doped TiO_2/C nanocomposites with high visible light photocatalytic activity. Nanoscale 4(2):576–584
74. Zuo F, Bozhilov K, Dillon RJ et al (2012) Active facets on titanium (III)-doped TiO_2: an effective strategy to improve the visible-light photocatalytic activity. Angew Chem 124 (25):6327–6330
75. Zhao L, Chen X, Wang X et al (2010) One-step solvothermal synthesis of a carbon@TiO_2 dyade structure effectively promoting visible-light photocatalysis. Adv Mater 22 (30):3317–3321
76. Liu G, Zhao Y, Sun C et al (2008) Synergistic effects of B/N doping on the visible-light photocatalytic activity of mesoporous TiO_2. Angew Chem Int Ed 47(24):4516–4520
77. Xing MY, Li WK, Wu YM et al (2011) Formation of new structures and their synergistic effects in boron and nitrogen codoped TiO_2 for enhancement of photocatalytic performance. J Phys Chem C 115(16):7858–7865
78. Hopper EM, Sauvage F, Chandiran AK et al (2012) Electrical properties of Nb-, Ga-, and Y-substituted Nanocrystalline Anatase TiO_2 prepared by hydrothermal synthesis. J Am Ceram Soc 95(10):3192–3196
79. Cong Y, Zhang J, Chen F et al (2007) Preparation, photocatalytic activity, and mechanism of nano-TiO_2 co-doped with nitrogen and iron (III). J Phys Chem C 111(28):10618–10623
80. Zielińska A, Kowalska E, Sobczak JW et al (2010) Silver-doped TiO_2prepared by microemulsion method: surface properties, bio-and photoactivity. Sep Purif Technol 72 (3):309–318
81. Sakthivel S, Kisch H (2003) Daylight photocatalysis by carbon-modified titanium dioxide. Angew Chem Int Ed 42(40):4908–4911
82. Wu Y, Liu H, Zhang J et al (2009) Enhanced photocatalytic activity of nitrogen-doped titania by deposited with gold. J Phys Chem C 113(33):14689–14695

83. Xing M, Zhang J, Chen F (2009) Photocatalytic performance of N-doped TiO_2 adsorbed with Fe^{3+} ions under visible light by a redox treatment. J Phys Chem C 113(29):12848–12853
84. Yu JC, Yu J, Ho W et al (2002) Effects of F-doping on the photocatalytic activity and microstructures of nanocrystalline TiO_2 powders. Chem Mater 14(9):3808–3816
85. Goswami P, Ganguli JN (2012) Evaluating the potential of a new titania precursor for the synthesis of mesoporous Fe-doped titania with enhanced photocatalytic activity. Mater Res Bull 47(8):2077–2084
86. Justicia I, Ordejón P, Canto G et al (2002) Designed self-doped titanium oxide thin films for efficient visible-light Photocatalysis. Adv Mater 14(19):1399–1402
87. Cao Y, Yang W, Zhang W et al (2004) Improved photocatalytic activity of Sn^{4+} doped TiO_2 nanoparticulate films prepared by plasma-enhanced chemical vapor deposition. New J Chem 28(2):218–222
88. Kurtz SR, Gordon RG (1987) Chemical vapor deposition of doped TiO_2 thin films. Thin Solid Films 147(2):167–176
89. Su Y, Zhang X, Han S et al (2007) F–B-codoping of anodized TiO_2 nanotubes using chemical vapor deposition. Electrochem Commun 9(9):2291–2298
90. Navío J, Colón G, Litter MI et al (1996) Synthesis, characterization and photocatalytic properties of iron-doped titania semiconductors prepared from TiO_2 and iron (III) acetylacetonate. J Mol Catal A Chem 106(3):267–276
91. Yu J, Xiang Q, Zhou M (2009) Preparation, characterization and visible-light-driven photocatalytic activity of Fe-doped titania nanorods and first-principles study for electronic structures. Appl Catal B Environ 90(3):595–602
92. Surolia PK, Tayade RJ, Jasra RV (2007) Effect of anions on the photocatalytic activity of Fe (III) salts impregnated TiO_2. Ind Eng Chem Res 46(19):6196–6203
93. Di Paola A, Marci G, Palmisano L et al (2002) Preparation of polycrystalline TiO_2 photocatalysts impregnated with various transition metal ions: characterization and photocatalytic activity for the degradation of 4-nitrophenol. J Phys Chem B 106(3):637–645
94. Chen X, Liu L, Peter YY et al (2011) Increasing solar absorption for photocatalysis with black hydrogenated titanium dioxide nanocrystals. Science 331(6018):746–750
95. Naldoni A, Allieta M, Santangelo S et al (2012) Effect of nature and location of defects on bandgap narrowing in black TiO_2 nanoparticles. J Am Chem Soc 134(18):7600–7603
96. Xia T, Zhang C, Oyler NA et al (2013) Hydrogenated TiO_2 nanocrystals: a novel microwave absorbing material. Adv Mater 25(47):6905–6910
97. Chen X, Liu L, Liu Z et al (2013) Properties of disorder-engineered black titanium dioxide nanoparticles through hydrogenation. Sci Rep 3
98. Khan SU, Al-Shahry M, Ingler WB (2002) Efficient photochemical water splitting by a chemically modified n-TiO_2. Science 297(5590):2243–2245
99. In S, Orlov A, Berg R et al (2007) Effective visible light-activated B-doped and B, N-codoped TiO_2photocatalysts. J Am Chem Soc 129(45):13790–13791
100. Xia T, Zhang W, Murowchick JB et al (2013) A facile method to improve the photocatalytic and lithium-ion rechargeable battery performance of TiO_2 nanocrystals. Adv Energy Mater 3 (11):1516–1523
101. Wang Z, Yang C, Lin T et al (2013) H-doped black Titania with very high solar absorption and excellent photocatalysis enhanced by localized surface plasmon resonance. Adv Funct Mater 23(43):5444–5450
102. Kurosu H, Yamanobe T (2012) A specialist periodical report on nuclear magnetic resonance (2011/8) synthetic macromolecules. Specialist Periodical Reports- Nucl Magn Res 41:386
103. Choi W, Termin A, Hoffmann MR (1994) The role of metal ion dopants in quantum-sized TiO_2: correlation between photoreactivity and charge carrier recombination dynamics. J Phys Chem 98(51):13669–13679
104. Zhang J, Xu LJ, Zhu ZQ et al (2015) Synthesis and properties of (Yb, N)-TiO_2 photocatalyst for degradation of methylene blue (MB) under visible light irradiation. Mater Res Bull 70:358–364

105. Zhu J, Zheng W, He B et al (2004) Characterization of Fe–TiO_2 photocatalysts synthesized by hydrothermal method and their photocatalytic reactivity for photodegradation of XRG dye diluted in water. J Mol Catal A Chem 216(1):35–43
106. Zhu J, Chen F, Zhang J et al (2006) Fe^{3+}-TiO_2 photocatalysts prepared by combining sol–gel method with hydrothermal treatment and their characterization. J Photochem Photobiol A Chem 180(1):196–204
107. Xiao L, Zhang J, Cong Y et al (2006) Synergistic effects of doped Fe^{3+} and deposited Au on improving the photocatalytic activity of TiO_2. Catal Lett 111(3):207–211
108. Wu Y, Zhang J, Xiao L et al (2009) Preparation and characterization of TiO_2photocatalysts by Fe^{3+} doping together with Au deposition for the degradation of organic pollutants. Appl Catal B Environ 88(3):525–532
109. You X, Chen F, Zhang J et al (2005) A novel deposition precipitation method for preparation of Ag-loaded titanium dioxide. Catal Lett 102(3):247–250
110. Wang W, Zhang J, Chen F et al (2008) Preparation and photocatalytic properties of Fe^{3+}-doped Ag@TiO_2 core–shell nanoparticles. J Colloid Interface Sci 323(1):182–186
111. Jaiswal R, Patel N, Kothari DC et al (2012) Improved visible light photocatalytic activity of TiO_2 co-doped with Vanadium and Nitrogen. Appl Catal B Environ 126:47–54
112. Sun L, Zhao X, Cheng X et al (2012) Synergistic effects in La/N co-doped TiO_2 anatase (101) surface correlated with enhanced visible-light photocatalytic activity. Langmuir 28 (13):5882–5891
113. Yuan S, Sheng Q, Zhang J et al (2006) Synthesis of Pd nanoparticles in La-doped mesoporous titania with polycrystalline framework. Catal Lett 107(1):19–24
114. Chen QL, Wang Y, Zhong CY et al (2011) Effect of Co-doped La^{3+}/halogen on visible light photocatalytic activity of TiO_2. Trans Tech Publ 239:1923–1928
115. Anandan S, Ikuma Y, Murugesan V (2012) Highly active rare-earth-metal La-doped photocatalysts: fabrication, characterization, and their photocatalytic activity. Int J Photoenerg 2012:1
116. Ma Y, Xing M, Zhang J et al (2012) Synthesis of well ordered mesoporous Yb, N co-doped TiO_2 with superior visible photocatalytic activity. Microporous Mesoporous Mater 156:145–152
117. Ma Y, Zhang J, Tian B et al (2012) Synthesis of visible light-driven Eu, N co-doped TiO_2 and the mechanism of the degradation of salicylic acid. Res Chem Intermed 38(8):1947–1960
118. Ma Y, Zhang J, Tian B et al (2010) Synthesis and characterization of thermally stable Sm, N co-doped $TiO_2$with highly visible light activity. J Hazard Mater 182(1):386–393
119. Zhao Y, Liu J, Shi L et al (2011) Solvothermal preparation of Sn4+ doped anatase TiO_2nanocrystals from peroxo-metal-complex and their photocatalytic activity. Appl Catal B Environ 103(3):436–443
120. Xiufeng Z, Juan L, Lianghai L et al (2011) Preparation of crystalline Sn-doped $TiO_2$and its application in visible-light photocatalysis. J Nanomater 2011:47
121. Lu G, Linsebigler A, Jr Y et al (1994) Ti3+ defect sites on TiO_2(110): production and chemical detection of active sites. J Phys Chem 98(45):11733–11738
122. Sasikala R, Shirole A, Sudarsan V et al (2009) Highly dispersed phase of SnO2 on TiO_2nanoparticles synthesized by polyol-mediated route: photocatalytic activity for hydrogen generation. Int J Hydrog Energy 34(9):3621–3630
123. Nakamura I, Negishi N, Kutsuna S et al (2000) Role of oxygen vacancy in the plasma-treated TiO_2photocatalyst with visible light activity for NO removal. J Mol Catal A Chem 161 (1):205–212
124. Linsebigler AL, Lu G, Jr Y (1995) Photocatalysis on TiO_2surfaces: principles, mechanisms, and selected results. Chem Rev 95(3):735–758
125. Nagaveni K, Hegde MS, Ravishankar N et al (2004) Synthesis and structure of nanocrystalline $TiO_2$with lower band gap showing high photocatalytic activity. Langmuir 20(7):2900–2907
126. Kamisaka H, Adachi T, Yamashita K (2005) Theoretical study of the structure and optical properties of carbon-doped rutile and anatase titanium oxides. J Chem Phys 123(8):084704

127. Bai H, Liu Z, Sun DD (2012) Facile preparation of monodisperse, carbon doped single crystal rutile TiO_2nanorod spheres with a large percentage of reactive (110) facet exposure for highly efficient H2 generation. J Mater Chem 22(36):18801–18807
128. Yu J, Dai G, Xiang Q et al (2011) Fabrication and enhanced visible-light photocatalytic activity of carbon self-doped TiO_2sheets with exposed {001} facets. J Mater Chem 21 (4):1049–1057
129. Lin X, Rong F, Ji X et al (2011) Carbon-doped mesoporous TiO_2film and its photocatalytic activity. Microporous Mesoporous Mater 142(1):276–281
130. Czoska AM, Livraghi S, Chiesa M et al (2008) The nature of defects in fluorine-doped TiO2. J Phys Chem C 112(24):8951–8956
131. Fattori A, Peter LM, Wang H et al (2010) Fast hole surface conduction observed for indoline sensitizer dyes immobilized at fluorine-doped tin oxide− TiO_2 surfaces. J Phys Chem C 114 (27):11822–11828
132. Shifu C, Yunguang Y, Wei L (2011) Preparation, characterization and activity evaluation of TiN/F-TiO_2 photocatalyst. J Hazard Mater 186(2):1560–1567
133. Ma HL, Zhang DH, Win SZ et al (1996) Electrical and optical properties of F-doped textured SnO_2 films deposited by APCVD. Sol Energy Mater Sol Cells 40(4):371–380
134. Minami T (2000) New n-type transparent conducting oxides. MRS Bull 25(8):38–44
135. Rakhshani AE, Makdisi Y, Ramazaniyan HA (1998) Electronic and optical properties of fluorine-doped tin oxide films. J Appl Phys 83(2):1049–1057
136. Cui Y, Du H, Wen LS et al (2009) Investigation of electronic structures of F-doped TiO_2 by first-principles calculation. Trans Tech Publ 620:647–650
137. Liu B, Gu M, Liu X et al (2010) First-principles study of fluorine-doped zinc oxide. Appl Phys Lett 97(12):122101
138. Gonzalez-Hernandez R, Martinez AI, Falcony C et al (2010) Study of the properties of undoped and fluorine doped zinc oxide nanoparticles. Mater Lett 64(13):1493–1495
139. Zhao W, Ma W, Chen C et al (2004) Efficient degradation of toxic organic pollutants with Ni_2O_3/TiO_2-x B x under visible irradiation. J Am Chem Soc 126(15):4782–4783
140. Moon SC, Mametsuka H, Suzuki E et al (1998) Characterization of titanium-boron binary oxides and their photocatalytic activity for stoichiometric decomposition of water. Catal Today 45(1):79–84
141. Chen D, Yang D, Wang Q et al (2006) Effects of boron doping on photocatalytic activity and microstructure of titanium dioxide nanoparticles. Ind Eng Chem Res 45(12):4110–4116
142. Jung KY, Park SB, Ihm SK (2004) Local structure and photocatalytic activity of B_2O_3–SiO_2/ TiO_2 ternary mixed oxides prepared by sol–gel method. Appl Catal B Environ 51(4):239–245
143. Xing M, Wu Y, Zhang J et al (2010) Effect of synergy on the visible light activity of B, N and Fe co-doped $TiO_2$for the degradation of MO. Nanoscale 2(7):1233–1239
144. Wu Y, Xing M, Zhang J (2011) Gel-hydrothermal synthesis of carbon and boron co-doped $TiO_2$and evaluating its photocatalytic activity. J Hazard Mater 192(1):368–373
145. Naik B, Parida KM (2010) Solar light active photodegradation of phenol over a Fe x Ti1−xO_2−yNy Nanophotocatalyst. Ind Eng Chem Res 49(18):8339–8346
146. Wang W, Lu C, Ni Y et al (2012) Preparation and characterization of visible-light-driven N–F–Ta tri-doped TiO_2 photocatalysts. Appl Surf Sci 258(22):8696–8703
147. Cong Y, Chen F, Zhang J et al (2006) Carbon and nitrogen-codoped TiO_2 with high visible light photocatalytic activity. Chem Lett 35(7):800–801
148. Gombac V, De Rogatis L, Gasparotto A et al (2007) TiO_2 nanopowders doped with boron and nitrogen for photocatalytic applications. Chem Phys 339(1):111–123
149. Komai Y, Okitsu K, Nishimura R et al (2011) Visible light response of nitrogen and sulfur co-doped TiO_2 photocatalysts fabricated by anodic oxidation. Catal Today 164(1):399–403
150. Yang G, Xiao T, Sloan J et al (2011) Low-temperature synthesis of visible-light active fluorine/sulfur Co-doped mesoporous TiO_2 microspheres. Chem Eur J 17(4):1096–1100

151. Wu Y, Xing M, Tian B et al (2010) Preparation of nitrogen and fluorine co-doped mesoporous TiO_2 microsphere and photodegradation of acid orange 7 under visible light. Chem Eng J 162 (2):710–717
152. Wei H, Wu Y, Lun N et al (2004) Preparation and photocatalysis of TiO_2 nanoparticles co-doped with nitrogen and lanthanum. J Mater Sci 39(4):1305–1308
153. Khan R, Kim SW, Kim TJ et al (2008) Comparative study of the photocatalytic performance of boron–iron Co-doped and boron-doped TiO_2 nanoparticles. Mater Chem Phys 112 (1):167–172
154. Wei F, Zhu T (2007) Preparation and photocatalytic property of S and Fe co-doped TiO_2 nanoparticles. Appl Chem Ind 36:421–424
155. Devi LG, Nagaraj B, Rajashekhar KE (2012) Synergistic effect of Ag deposition and nitrogen doping in TiO_2 for the degradation of phenol under solar irradiation in presence of electron acceptor. Chem Eng J 181:259–266